

# PHYSICAL REVIEW LETTERS

VOLUME 45

8 SEPTEMBER 1980

NUMBER 10

## Muoproduction of Neutral Strange Hadrons at 225 GeV

R. G. Hicks, H. L. Anderson, N. E. Booth, W. R. Francis, B. A. Gordon, W. W. Kinnison,  
T. B. W. Kirk, W. A. Loomis, H. S. Matis, L. W. Mo, L. C. Myriantopoulos,  
F. M. Pipkin, J. Proudfoot, T. W. Quirk, A. L. Sessoms, W. D. Shambroom,  
A. Skuja, M. A. Staton, C. Tao, W. S. C. Williams,

Richard Wilson, and S. C. Wright

*High Energy Physics Laboratory and Department of Physics, Harvard University, Cambridge, Massachusetts 02138, and Enrico Fermi Institute and University of Chicago, Chicago, Illinois 60637, and Fermilab, Batavia, Illinois 60510, and Department of Physics, The University of Illinois at Urbana-Champaign, Urbana, Illinois 61801, and Department of Physics and Astronomy, University of Maryland, College Park, Maryland 20742, and Physics Department, Michigan State University, East Lansing, Michigan 48824, and Department of Nuclear Physics, The University of Oxford, Oxford OX1 3RH, England, and Physics Department, Virginia Polytechnic Institute and State University,*

*Blacksburg, Virginia 24061*

(Received 14 April 1980)

The production of  $K_s^0$ ,  $\Lambda^0$ , and  $\bar{\Lambda}^0$  has been measured in deep-inelastic muon scattering at 225 GeV; decays into two charged hadrons were detected. Momentum distributions are compared to the inclusive charged-hadron distributions measured in the same experiment. The range of virtual-photon parameters covered is  $0.4 < Q^2 < 50 \text{ GeV}^2$  and  $20 < \nu < 210 \text{ GeV}$ .

PACS numbers: 13.60.Kd, 13.60.Rj

We report further results from the deep-inelastic muon scattering experiments at Fermilab. Previous papers have presented our measurements of the inclusive muon cross section, structure functions  $\nu W_2(Q^2, \nu)$ , and the ratio  $R = \sigma_L/\sigma_T$ ,<sup>1</sup> and of charged-hadron production.<sup>2</sup> In this Letter, we describe the production of the neutral strange particles  $K_s^0$ ,  $\Lambda^0$ , and  $\bar{\Lambda}^0$  in muon-proton collisions, detected by their decay into two oppositely charged hadrons.

A complete description of the apparatus in its 225-GeV configuration has been published elsewhere.<sup>1</sup> The beam consists of positive muons at an energy of  $219 \pm 8.5 \text{ GeV}$  and an intensity of  $(1.2-1.3) \times 10^6/\text{sec}$ , incident on a 120-cm-long liquid-hydrogen target ( $8.5 \text{ g/cm}^2$ ). The total effective flux for these data is  $7.44 \times 10^{10}$  muons,

with 36 000 analyzed triggers for  $Q^2 > 0.4$ . The  $Q^2$  lower limit was imposed to suppress electromagnetic events. Figure 1 is an unweighted scatter plot of  $Q^2$  and  $\nu$  for the events containing  $K_s^0$  or  $\Lambda^0$ .

Below about 8 GeV, charged particles produced in the target will be swept out of the downstream spark chambers by the spectrometer magnet and cannot be detected by these chambers; the presence of 12 multiwire proportional chamber (MWPC) planes within the magnet, however, allows us to reconstruct curved tracks and analyze particles with momenta down to about 1 GeV; below 2 GeV, the detection efficiency drops off rapidly. The low-energy detection ability enables us to detect a significant fraction of  $V^0$  decays.

The steps taken to extract  $V^0$  decays from the total sample of good muon-scattering events are

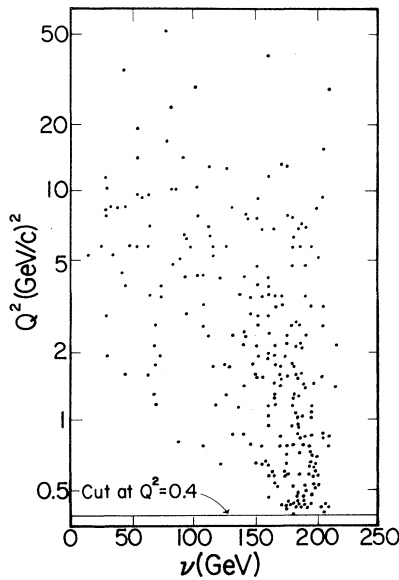


FIG. 1. Scatter plot of  $Q^2, \nu$  for events having one or more  $K_s^0$  or  $\Lambda^0$ , with  $Q^2 > 0.4$ .

as follows. For each pair of oppositely charged tracks, the distance of closest approach (dca) is calculated; the maximum allowed is 1 cm. We measure the distance between the muon vertex and the neutral pair vertex, and calculate the associated uncertainty (standard deviation). We require the pair vertex to be at least 2.5 standard deviations downstream from the muon vertex. We also require the momentum vector for the pair to point backwards to the muon vertex within 1.25 cm in the transverse plane.

In the absence of particle identification, each neutral pair can contribute to three mass plots, corresponding to the decays  $K_s^0 \rightarrow \pi^+\pi^-$ ,  $\Lambda^0 \rightarrow p\pi^-$ , and  $\bar{\Lambda}^0 \rightarrow \bar{p}\pi^+$ . A phase-space calculation is used to correct the mass spectra for pairs which can be either  $K_s^0$  or  $\Lambda^0$ , and they are assigned on a statistical basis. The calculation shows them to be almost all  $\Lambda^0$  and  $\bar{\Lambda}^0$ .

Finally, we make what is essentially an opening-angle cut to reduce background. It is required that the decay angle  $\theta_{c.m.}$  in the decaying particle's center of mass satisfy  $|\cos\theta_{c.m.}| \leq 0.9$ . As  $\cos\theta_{c.m.}$  is uniformly distributed for spin-0 particles, this excludes 10% of real decays, but reduces the background by ~42%. Figure 2 shows the  $\pi^+\pi^-$  mass spectrum after these cuts, compared to the same procedure applied to same-sign pairs. The  $K_s^0$  peak has a signal/background ratio of 3.5. Because we have to include the hy-

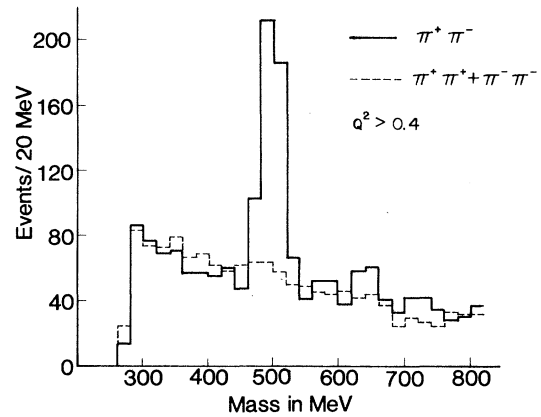


FIG. 2.  $\pi^+\pi^-$  mass spectrum for good  $V^0$  events, compared to the sum of same-sign pairs. These yields are not renormalized.

drogen target in our decay space, reinteracting hadrons and  $\delta$  rays contribute to the background.

As a check on our results we calculate the mass and lifetime of each  $K_s^0$  that we detect. This requires a background subtraction which can be done two ways, by subtracting events from either side of the peak or by subtracting same-sign events. Both methods give the same results within statistics and the following data use the same-sign background subtraction. Our  $K_s^0$  mass resolution (1 standard deviation) is 13 MeV, and we find a mass of  $495.8 \pm 0.8$  MeV, compared with the published value of  $497.70 \pm 0.13$  MeV.<sup>3</sup> This serves as a check on our momentum calibration. Figure 3 shows the distribution of

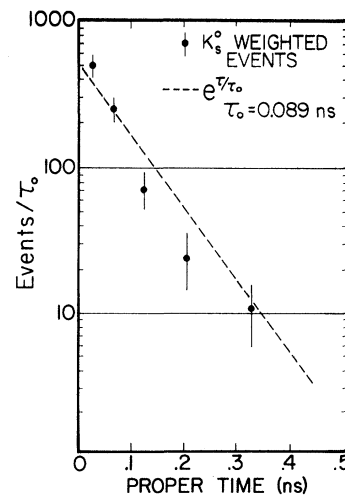


FIG. 3. Proper-time distribution for  $K_s^0$ , with same-sign background subtracted. Dotted line is based on published lifetime.

TABLE I. Number of strange neutral hadrons detected (unweighted). Only statistical errors are indicated.

	$K_s^0$	$\Lambda$	$\bar{\Lambda}$
Total events in peak	472 ± 21.8	288 ± 17.0	285 ± 17.0
Background	105 ± 10.2	130 ± 11.5	130 ± 11.5
Signal	367 ± 24.0	158 ± 20.4	155 ± 20.4
Signal	3.50 ± 0.39	1.21 ± 0.15	1.19 ± 0.15
Background			

proper lifetimes for the observed events. The dashed line has a slope determined by the published lifetime measurements<sup>3</sup> of the  $K_s^0$ . The  $\chi^2$  is 12.1 for five degrees of freedom.

Similar results are obtained for the  $\Lambda^0, \bar{\Lambda}^0$  mass and lifetime. Here, however, the background subtraction is subject to much greater systematic uncertainty. Since the  $\Lambda^0$  mass peak is so near the low-mass end of the spectrum, and given our experimental mass resolution, background subtraction for the  $\Lambda^0, \bar{\Lambda}^0$  data is based solely on subtraction of like-spin pairs. The overall normalization of the number of  $\Lambda^0$  and  $\bar{\Lambda}^0$  has an estimated 25% systematic error. Table I shows the number of particles of each type detected, and the statistical errors only.

Figure 4 presents the longitudinal structure functions of  $K_s^0$  and  $\Lambda^0$  production.  $D_h(z)$  is the number of hadrons of type  $h$  produced per unit  $z$  per interacting muon, where  $z = E_h/\nu$  is the hadron's fraction of the virtual-photon energy.  $D_h(z)$  for the neutral strange hadrons has been corrected for all acceptance and efficiency cuts and for the  $K_s^0$  and  $\Lambda^0$  branching ratios into two charged hadrons. The solid lines represent our results for the inclusive charged hadrons, multiplied by a factor of 0.10 to bring them into scale.<sup>2</sup>  $D_h^+(z)$  for all hadrons has a much steeper slope at low  $z$ , giving smaller  $K_s^0/\pi$  and  $\Lambda^0/\pi$  ratios in the target fragmentation ( $z < 0.2$ ) region than in the photon fragmentation region. We also show data from an electron-proton experiment,<sup>4</sup> which had somewhat better statistics for  $K_s^0$  production,

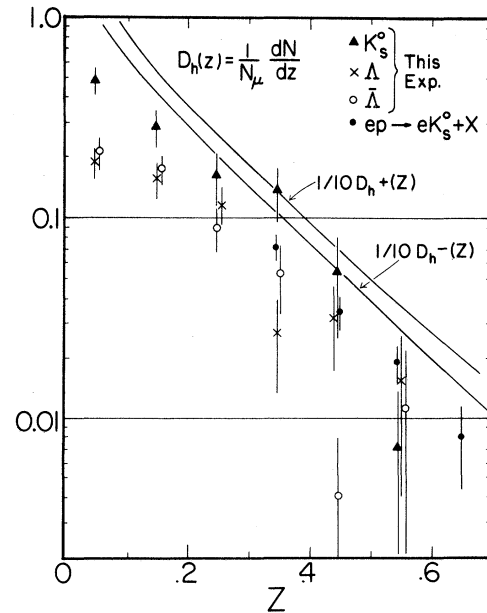


FIG. 4.  $D_h(z)$  for  $K_s^0, \Lambda^0$ , and  $\bar{\Lambda}^0$ , where  $D(z) = N_\mu^{-1} dN_h/dz$ . The electron data are from Ref. 4; the lines for  $h^+$  and  $h^-$  are eyeball fits to data from this experiment.

but limited to  $z > 0.3$ . Our results are consistent with the electroproduction data.

We find that strange-particle production depends on  $Q^2$  and  $s$  only for small  $z$ . The available statistics do not allow us to separate  $Q^2$  and  $s$  effects independently; it should be noted that high- $Q^2$  events tend to have lower average  $s$ . In Fig. 5 we display  $D(z)$  for  $K_s^0$  in two different  $Q^2$  regions; Table II gives average  $Q^2, s$ , and  $\langle p_T^2 \rangle$  for these two regions, and the integral  $\int_0^1 D(z) dz$ , which is the number of  $K_s^0$  per virtual photon.

In the usual quark-parton picture, the transverse momentum relative to the virtual-photon direction of hadrons produced in deep-inelastic interactions is due to a combination of initial transverse momenta of the partons and the transverse momentum imparted by the quark fragmentation process. Figure 6 shows the mean transverse momentum squared for hadrons as a func-

TABLE II. Comparison of  $K_s^0$  properties for two ranges of  $Q^2$ .

	$\langle Q^2 \rangle$ (GeV <sup>2</sup> )	$\langle s \rangle$ (GeV <sup>2</sup> )	$\langle p_T^2 \rangle$ (GeV <sup>2</sup> )	$\int_0^1 D(z) dz$
$0.4 < Q^2 < 2$	0.94	324	0.256 ± 0.045	0.129 ± 0.015
$Q^2 > 2$	7.04	224	0.350 ± 0.049	0.095 ± 0.013

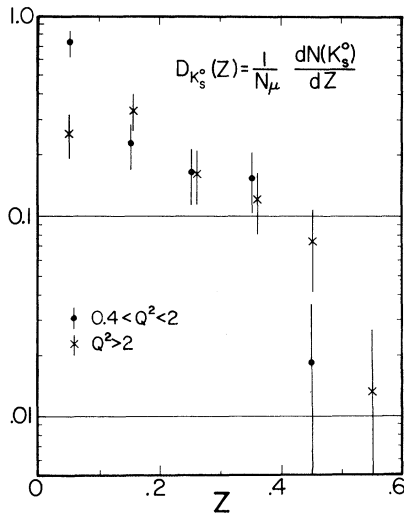


FIG. 5.  $D(z)$  for  $K_s^0$  in two  $Q^2$  bins.

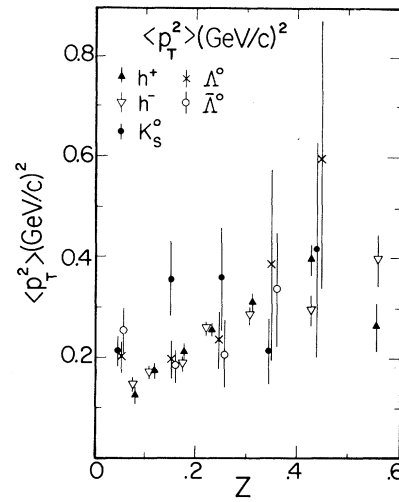


FIG. 6. Average transverse momentum squared for  $K_s^0$  and  $\Lambda^0$ ;  $h^\pm$  points are from Ref. 2.

tion of  $z$ . We observe that the  $K_s^0$  and  $\Lambda^0$  appear to have a slightly higher average  $p_T^2$  than the charged hadrons, and exhibit a similar rise as  $z$  increases. Again, our data are consistent with the lower-energy electroproduction results, which had a  $\langle p_T^2 \rangle$  for the  $K_s^0$  of  $0.233 \pm 0.028 \text{ GeV}^2$ .

In the usual quark-parton model, the strange quarks in  $K$  and  $\Lambda$  production come from gluon-produced  $q\bar{q}$  pairs; thus observed differences between strange and nonstrange hadrons are manifestations of the differences between valence quarks and gluons. The expected higher  $\langle p_T^2 \rangle$  of the latter is one example of such a difference. Without an exact method of calculating the effects of gluon bremsstrahlung and quark dressing functions, however, it is not possible to make more than a rough estimate of these underlying quantities.

We wish to thank Dr. G. Ascoli and Dr. M. Shupe,

who supplied us with sophisticated reconstruction programs. J. MacAllister helped process much of the raw data on the computer at Rutherford Laboratory. We are also indebted to the staff of the Neutrino Department at Fermilab and to the staffs at our home institutions.

This research was supported by the National Science Foundation under Contract No. PHY-71-02186-A05, by the U. S. Department of Energy under Contracts No. EY-76-C-02-3064 and No. E(11-1)-1195, and by the Science Research Council (United Kingdom).

<sup>1</sup>B. A. Gordon *et al.*, Phys. Rev. D **20**, 2645 (1979).

<sup>2</sup>W. A. Loomis *et al.*, Phys. Rev. D **19**, 2543 (1979).

<sup>3</sup>C. Bricman *et al.*, Phys. Lett. **75B**, 2 (1978).

<sup>4</sup>I. Cohen *et al.*, Phys. Rev. Lett. **40**, 1614 (1978).